Screening of strong bicarbonate forming solvents for CO$_2$ capture

Hartono[1], A., Vevelstad[2], S.J., Ciftja[1], A., and Knuutila[1]*, H.K.

[1]Department of Chemical Engineering, Norwegian University of Science and Technology,

N-7491 Trondheim, Norway

[2]SINTEF, Materials and Chemistry, P.B. 4760, 7465 Trondheim, Norway

* To whom correspondence should be addressed, Phone: +47-73594100, Fax: +47-73594080, e-mail:

hanna.knuutila@ntnu.no

Keywords: Screening, Bicarbonate forming solvent, CO$_2$ capture, dissociation constant

Abstract

Fifteen bicarbonate forming solvents were tested and compared to 30 mass% MEA using a screening apparatus. Additionally the pKa values of each of the solvents at room temperature were measured. The overall evaluation was based on screening tests allowing estimation of cyclic capacity, pKa measurements and operative behavior of the system (foaming, high viscosity, precipitation). Based on the overall evaluation, two solvents, 2-PPE and 1-(2HE)PRLD, were chosen for further characterization. The solvent concentration was optimized using the screening setup. The optimal solvent concentrations found were 50 mass% 2-PPE, and 40 mass% 1-(2HE)PRLD.

1. Introduction

Absorption using chemical absorbents has been widely used for acid gas removal in natural gas industry for over 60 years. The best absorbents are the ones with high net cyclic capacity (high absorption and desorption rates are necessary), fast reaction/absorption rates for CO_2, low heat of reaction, high chemical stability, low vapor pressure and low corrosiveness. Several different types of amine have been used such as alkanolamines and polyamines. Alkanolamines are widely used as solvents for post-combustion CO_2- capture because the compounds have two functional groups which in combination give an increase of CO_2 solubility in water and thus higher absorption of CO_2 (Kohl and Nielsen, 1997). The most common alkanolamines studied for this purpose are 2-ethanolamine (MEA, CAS 141-43-5), diethanolamine (DEA, CAS 111-42-2), N-methyldiethanol-amine (MDEA, CAS 105-59-9), 2-amino-2-methylpropanol (AMP, CAS 124-68-5) and blends of these. Of the polyamines, piperazine has received attention during the last five years (Chen et al., 2013; Freeman et al., 2010; Nielsen et al., 2013).

In chemical absorption, CO_2 is bound as bicarbonate or carbamate. The formation reaction for the bicarbonate is given in reaction R_1 and for the carbamate in reaction R_2:

$$CO_{2(aq)} + H_2O + R_3N \leftrightarrow HCO_3^- + R_3NH^+ \tag{R_1}$$

Where R_3N can be any amine component.

$$CO_{2(aq)} + R_2NH + R_3N \leftrightarrow R_2NCO_2^- + R_3NH^+ \tag{R_2}$$

The base strength of the amine (R_3) determines the extent of bicarbonate formation of an amine:

$$R_3N + H_3O^+ \leftrightarrow R_3NH^+ + H_2O \tag{R_3}$$

Carbamate formation depends on the stability of the carbamate, which is expressed by the equilibrium given in reaction R_4, and the base strength (R_3).

$$HCO_3^- + R_2NH \leftrightarrow R_2NCO_2^- + H_2O \tag{R_4}$$

The CO_2 absorption capacity is lower for amines forming stable carbamates since two amine molecules participate in the reaction with one CO_2 molecule (see reaction R_2). CO_2 absorption could be

increased by hydrolysis of the carbamate. The degree of hydrolysis depends on amine concentration, pH of the solution and chemical stability of the carbamate (Caplow, 1968; Chakraborty et al., 1988; Ewing et al., 1980; Hook, 1997)

Carbamate stabilities and basicity of the amines are the two main equilibrium constants which to a large extent determine how a solvent will perform in CO_2 absorption (da Silva, 2011). A solution with higher bicarbonate ratio is expected to have higher CO_2 capacity, faster desorption rate and to give a leaner solution (Hook, 1997; Sartori and Savage, 1983).

Over the years several studies regarding the influence of amine structure on capacity for CO_2 capture as well as CO_2 absorption and desorption rate and carbamate stability have been performed (Bonenfant et al., 2003; Chakraborty et al., 1986; Chowdhury et al., 2009; Chowdhury et al., 2011; Chowdhury et al., 2013a; Chowdhury et al., 2013b; da Silva and Svendsen, 2006, 2007; Fernandes et al., 2012; Robinson et al., 2012; Sartori and Savage, 1983; Singh et al., 2009; Yang et al., 2012). The studies have discussed different factors as basicity, the pH, of the solution polarity and steric hindrance/structural characteristics of the compound (Bonenfant et al., 2003; Sartori and Savage, 1983). However, it is also important to include electron density, hydrogen bonding and solvation since these systems have an abundance of amino lone pair, hydroxyl group ions and water (Yamada et al., 2013). A high CO_2 absorption capacity has been observed for amine forming an unstable carbamate. Several research groups have indicated that substituents at the α-carbon can create an unstable carbamate (Chakraborty et al., 1986; Chakraborty et al., 1988; McCann et al., 2011; Sartori and Savage, 1983), but this instability has been explained in different ways. Sartori et al. suggest that the instability is caused by the steric hindrance these substituent introduces while Chakraborty et al. discussed the change in electron density caused by the substituents which, in this particular case, was expected to reduce the charge at the nitrogen atom making it more susceptible to hydrolysis by the hydroxide in the solution (Chakraborty et al., 1986; Chakraborty et al., 1988; Singh et al., 2007).

Another important factor when selecting amine based absorbents for acid gas removal is acid and base strength represented respectively by the dissociation constant (pKa) and the basicity. There have been

several molecular modelling studies investigating basicity of solvents, pKa and temperature dependency of these factors (da Silva, 2005; da Silva and Svendsen, 2003; Gupta et al., 2012; Mergler et al., 2011; Yamada et al., 2010). Gas-phase basicities are related to solution-phase pKa by solvation free energies (Jackson et al., 2011) and from the quantum mechanical calculations by taking into account the hydrogen bonding in poly functional molecules (Bouchoux, 2007; Jackson et al., 2011; Karpas, 1992) showed a good agreement with experimental data (da Silva, 2005). In the work by da Silva (da Silva, 2005), the alkanolamines (MEA, DEA, 3-amino-1-propanol) and 1,2-ethanediol which were tested deviated from experimental values. Overall, the basicity and pKa of molecules can be explained based on evaluation of electron density e.g. charge density/dispersal, electronegativity, polarizability, resonance, substituents, orbitals, and aromaticity. The electron density are related to field and resonance effect where field effects operate through space electrostatic interaction and resonance effect operate through the π-electrons of the system (Carey and Sundberg, 2000).

When evaluating the amine performance for CO_2 capture shows that there is a trade-off between factors e.g. steric hindrance increases capacity while absorption rate is reduced and several factors that has been considered in literature when explaining the behavior observed during testing: molecular level (electron density), solution perspective (e.g. hydrogen bonding) or as in many cases from steric hindrance perspective.

To further investigate changes in performance, fifteen commercial, strong bicarbonate forming amines or amines interesting for correlating amine structure and solvent performance were tested in screening setup. The amines are given in Table 1. These amines were selected based on earlier experimental or modelling work conducted in several research environments e.g. RITE in Japan (Chowdhury et al., 2011; Chowdhury et al., 2013a; Chowdhury et al., 2013b; Goto et al., 2011a; Goto et al., 2011b), CSIRO in collaboration with the University of Newcastle in Australia (Fernandes et al., 2012; Puxty et al., 2009), Twente University and Procede Group BV (Singh et al., 2007, 2009) and NTNU (da Silva, 2005, 2011; da Silva and Svendsen, 2003; Gupta et al., 2012).

The new amines with different structure (ring, straight chain, variation in carbon chain and substituents) studied are expected to influence e.g. the bicarbonate ratio and pKa were tested. The amines are listed in Table 1. Steric hindrance effect on tBAE, IPAE, 3QUI, TMP-OL are expected to have high bicarbonate formation, particularly in tBAE, PAE and IPAE where different alkyl groups as steric hindrance (R-group) for amino group attached. It was already reported that PAE, IPAE, tBAE, 2PPM and 2PPE showed similar absorption rate as for MEA and may have lower heat of reaction (Chowdhury et al., 2011; Chowdhury et al., 2013a). DMAH, DEA-1P, DEA-1,2-PD, 1-(2HE)PP and 1-(2HE)PRLD reported to have moderate absorption rate, but high absorption capacity (Chowdhury et al., 2009; Chowdhury et al., 2013a). TM-1,4-DAB and DEAE-EO showed moderate absorption rate and low absorption capacity (Chowdhury et al., 2009; Chowdhury et al., 2013a), however they have structural features of interest and are therefore tested. DEAE-EO with ether group and TM-1,4-DAB with longer carbon chain between the amine molecules, the longer chain between amine molecules in polyamines has shown to increase the bicarbonate formation (Singh et al., 2007). Different structural features are also studied, such as: influence extra carbon between amino and alcohol function (DEEA and DEA-1P), influence of extra OH group (DEA-1,2-PD and DEA-1P), placement of substituents in the piperidine ring and carbon chain length between amine and alcohol function (1-(2HE)PP, 2-PPE and 2-PPM) and different ring size (1-(2HE)PP and 1-(2HE)PRLD). All tested solvent candidates have two different amine groups, i.e. secondary and tertiary. Secondary amines have the ability to form carbamate and bicarbonate. The ratio of carbamate to bicarbonate (Ciftja et al., 2014) must be very small for secondary amine to be considered as strong bicarbonate forming solvent. When the amount of carbamate formed is low, the absorption rate mostly depends on the bicarbonate carbamate formation, hence the system will also have low absorption rate.

2. Experimental Section

2.1. Chemicals

Commercially available chemicals used in this study are presented in Table 1 and without any further purification, 30 mass% amines in aqueous solutions were prepared by dissolving them into DI-water for screening experiment while for pKa measurement 0.01 mol of amines were dissolved in 1 kg DI-water. TMP-OL was observed to have low water solubility hence 11 mass% solution was prepared for screening test. IPAE has low purity therefore the impurities may strongly affect the results. A gravimetric procedure in the solution preparation was recorded with the MS6002S Scale (with an uncertainty $\pm 10^{-5} kg$).

Table 1. Chemicals used in this work

NO.	Chemical Name	Abbreviation	CAS No.	Formula	M (g/mol)	Phase*	Supplier	Purity (%min)
S1	Monoethanolamine	MEA	141-43-5	C_2H_7NO	61.08	Liquid	SA	99
S2	Diethanolamine	DEA	111-42-2	$C_4H_{11}NO$	105.14	Liquid	SA	98.5
S3	2-(Diethylamino)ethanol	DEEA	100-37-8	$C_6H_{15}NO$	117.19	Liquid	SA	99.5
1	2-(Isopropylamino)ethanol	IPAE	109-56-8	$C_5H_{13}NO$	103.16	Liquid	SA	70**
2	2-(Propylamino)ethanol	PAE	16369-21-4	$C_5H_{13}NO$	103.16	Liquid	SA	98
3	2-(tert-Butylamino)ethanol	tBAE	4620-70-6	$C_6H_{15}NO$	117.19	Solid	SA	99
4	2-Piperidinemethanol	2-PPM	3433-37-2	$C_6H_{13}NO$	115.17	Solid	SA	97
5	2-Piperidineethanol	2-PPE	1484-84-0	$C_7H_{15}NO$	129.20	Solid	SA	97
6	2,2,6,6-Tetramethyl-4-piperidinol	TMP-OL	2403-88-5	$C_9H_{19}NO$	157.25	Crystal	SA	98
7	Potassium Pipecolinic	KPIP	535-75-1	$C_6H_{11}NO_2$	129.16	Powder	SA	98
8	3-Diethylamino-1-propanol	DEA-1P	622-93-5	$C_7H_{17}NO$	131.22	Liquid	SA	97
9	3-(Diethylamino)-1,2-propanediol	DEA-1,2-PD	621-56-7	$C_7H_{17}NO_2$	147.22	Liquid	SA	98
10	N,N,N',N'-Tetramethyl-1,4-butanediamine	TM-1,4-DAB	111-51-3	$C_8H_{20}N_2$	144.26	Liquid	SA	98
11	2-(2-Diethylaminoethoxy)ethanol	DEAE-EO	140-82-9	$C_8H_{19}NO_2$	161.24	Liquid	TCI	98
12	6-Dimethylamino-1-hexanol	DMAH	1862-07-3	$C_8H_{19}NO$	145.24	Liquid	TCI	95
13	1-(2-Hydroxyethyl)pyrrolidine	1-(2HE)PRLD	2955-88-6	$C_6H_{13}NO$	115.17	Liquid	SA	97
14	1-(2-Hydroxyethyl)piperidine	1-(2HE)PP	3040-44-6	$C_7H_{15}NO$	129.20	Liquid	SA	99
15	3-Quinuclidinol	3QUI	1619-34-7	$C_7H_{13}NO$	127.18	Powder	SA	99
16	Carbon Dioxide	CO_2	124-38-9	CO_2	44.01	Gas	AGA	99.999
17	Nitrogen	N_2	7727-37-9	N_2	28.02	Gas	AGA	99.998
*) at ambient								
**) Impurity: 30% of N-isopropyl ethanolamine (N-Isopropyl-2-2'-iminodiethanol) CAS : 121-93-7								
SA = Sigma Aldrich TCI = Tokyo Chemical Industry								

2.2. Equipment and Procedures

Screening Apparatus:

The existing screening apparatus was used during the screening experiments (Aronu et al., 2011b; Aronu et al., 2010; Brúder et al., 2011; Hartono et al., 2014a; Ma'mun et al., 2007). The screening apparatus mimics an absorption (40°C and 95% CO_2 captured) and desorption (80°C and 90% CO_2 removal) processes in CO_2 capture plant and thus allows solvent performances estimation (rich/ lean

loading and cyclic capacity) of each solvent compared to the reference solvent(s). In this work MEA, DEA and DEEA were used as reference solvents. Additionally information related to foaming, solid formation and visible discoloration upon CO_2 loading may be gathered.

In this work a small ($\sim200\ cm^3$) jacketed glass reactor (OD= 70 mm, ID=4.5mm, H=135 mm) was used to reduce the solvent use and to better maintain a constant temperature during the experiments. Solvent amount (W_S) about ~0.125 kg recorded with MS6002S scale (uncertainty$\pm10^{-5}kg$) was introduced into the reactor. Bronkhorst® High-Tech mass flow controllers (MFC) of N$_2$ (0-5 NL/min, uncertainty 1% FS) and CO$_2$ (0-1 NL/min, uncertainty 1% FS) were used to adjust the feed gas composition at 10% of CO$_2$ and with total gas flow of 1NL/min. To improve the liquid-gas contact, a magnetic stirrer at 450 rpm was used. The gas leaving the reactor was cooled down with jacketed double-coils condensers (L=300mm, OD=58 mm). Any carry-over condensate was collected in a separation funnel connected in the bottom of the second condensers. An extra cold traps and a gas filter was installed to dry the gas before entering to a CO$_2$ analyzer. A Fisher–Rosemount BINOS® 100 NDIR CO$_2$ analyzer with 0-10% CO$_2$ in N$_2$ (uncertainty 1% FS) was used to measure CO$_2$ content in the gas outlet. When gas outlet concentration showed 9.5%, the absorption was finished while during the desorption process, 1.0% CO$_2$ was used as criteria of stoppage.

Liquid temperature in the reactor (uncertainty ±0.1°C) was controlled by a Lauda Ecoline E6 water bath. The screening setup is shown in Figure 1.

Based on the logged data the amount of CO$_2$ absorbed can be calculated using equation:

$$Q_{CO_2}\left(\frac{mol\ CO_2}{s}\right) = n_{CO_2}^{in} - \frac{x_{CO_2}^{Out}\cdot n_{N_2}^{In}}{1-x_{CO_2}^{Out}} \tag{1}$$

Where $n_{CO_2}^{in}(\frac{mol}{s})$ and $n_{N_2}^{In}(\frac{mol}{s})$ are the amounts of CO$_2$ and N$_2$ fed into the reactor, respectively and $x_{CO_2}^{Out}(-)$ is the volume % of CO$_2$ in the gas leaving the reactor. From this, the accumulated amount of CO$_2$ absorbed can then be integrated over period $dt(s)$:

$$N_{CO_2}(mol\ CO_2) = \int_0^t Q_{CO_2}\cdot dt \tag{2}$$

The absorption and stripping rates can be calculated from:

$$R_{CO_2} \left(\frac{mol\ CO_2}{kg\ solution \cdot s} \right) = \frac{1}{W_S} \cdot Q_{CO_2} \tag{3}$$

Where W_S ($kg\ solution$) is the amount of solvent in the reactor.

Finally, cyclic capacity and loading can be estimated from the equations (4) and (5).

$$Q_{cyc} \left(\frac{mol\ CO_2}{kg\ solution} \right) = \alpha_{Rich} - \alpha_{Lean} \tag{4}$$

The rich and lean loadings required in the previous equation are calculated from the total amount of CO_2 absorbed (giving $\alpha_{Rich}(\frac{mol}{kg\ solution})$) of from the total amount of CO_2 stripped (giving $\alpha_{Lean}(\frac{mol}{kg\ solution})$) by dividing these with the total amount of solvent:

$$\alpha \left(\frac{mol\ CO_2}{kg\ solution} \right) = \frac{N_{CO_2}}{W_S} \tag{5}$$

$n_{CO_2}^{in}, n_{N_2}^{In}$ and $x_{CO_2}^{Out}$ were recorded from the Mass Flow controller and the CO_2 analyzer respectively. Experimental procedures was verified and validated with a bench-marking solvent MEA 30 mass% (see Appendices A.1, Table A.1)
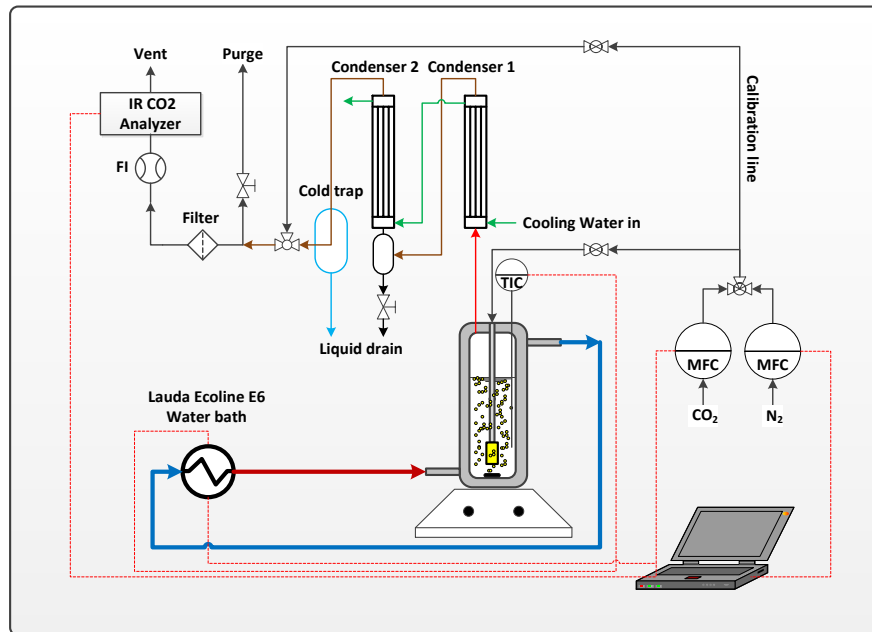
Figure 1: Screening Apparatus (MFC = Mass Flow Controller; TIC = Temperature Indicator and Controller); FI = Flow Indicator (Rotameter); IR = Infrared).

Dissociation constant:

The amine will react with any acid according to reaction (R$_3$) and the dissociation constant may then expressed as pKa according to:

$$K_a = \frac{a_{AmH^+} \cdot a_{H_2O}}{a_{Am} \cdot a_{H_3O^+}} \qquad (6)$$

This reaction can be observed in the pKa determining apparatus (Figure 2). The set up (Kim et al., 2011) consists of a Mettler Toledo G20 compact titration unit with a pH-electrode DSC-115 (uncertainty ± 0.02 pH), temperature sensor DT100 (uncertainty ± 0.1 °C) and a heating water bath Julabo M4 unit. A jacketed glass reactor (100 ml volume) wass connected to the heating circulator (temperature stability ± 0.1 °C). The glass pH-electrode was calibrated in advance at measuring temperature using buffer solutions traceable to the National Bureau of Standards (pH 4.01, 7.00, 9.21 and 11.0 from Mettler Toledo).

About 35 g of very dilute amine solution, concentration of 0.01 mol/kg H$_2$O, was titrated with 0.1 mol/l HCl solution. A dynamic equilibrium procedure provides an automatic adjustment of the amount HCl added into solution (minimum of 0.005 cm^3/min and maximum of 0.3 cm^3/min) to maintain a constant temperature (Hartono et al., 2014c). LabX 3.1 software provided by Mettler Toledo was used to calculate the pKa values as pH at half equivalence. At least duplicate experiments were performed. The pKa difference was small, less than 0.1%.
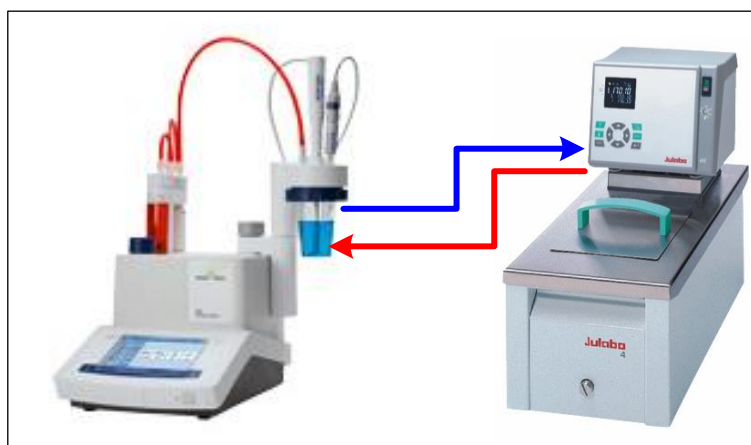
Figure 2: pKa apparatus set up.

<u>**Viscosities**</u>

Viscosities of rich and lean loadings were measured in a Rheometer Anton Paar MCR 100. The equipment and procedures were presented in Hartono et al. (2014b). The viscosity was calibrated with a D5 standard solvent (Paragon Scientific Ltd.) and the results were reproducible with an ARD value less than 1%.

3. Results and Discussion

3.1. Screening experiments

3.1.1. Secondary amines tested

In Table 2, the tested seven secondary amines are listed and in Figure 3 the absorption and desorption curves are shown. In the table some general observations, such foaming and solid formation during screening experiments are given. No solid formation nor viscosity issue was observed but some solvent showed tendencies to foam. Viscosities of rich and lean loadings are shown in Figure A.3 in Appendix A.3. The measured viscosities of MEA for both rich and lean loadings also agree well with Hartono et al. (2014b) with an ARD value less than 3%. The highest viscosity was observed for KPIP solvent (8.43 mPa.s) and the lowest one was observed for TMP-OL solvent (1.55 mPa.s), due to a low concentration use.

Foaming tendency was an issue for IPAE, TMP-OL and tBAE. To quantify the foaming tendency, a foaminess coefficient was estimated at experiment condition using the same method as in Thitakamol and Veawab (2008). The results are given in Appendix A.4. The foaming tendency might also be seen from the shape of the absorption curves in Figure 3. The results show that MEA derivate molecules which have tertiary or quaternary carbon attached to the amino group (i.e. IPAE and tBAE), with higher foaminess coefficient, tends to give more foaming than that attached in the secondary carbon, like PAE. Use a hydrophobicity parameter (Leo, 1991), which represent an association of non-polar groups or molecules in an aqueous environment, might explain foaming effect of different groups attached. For

example methyl group attached (-CH$_3$) to tertiary or quaternary carbon molecules has higher hydrophobicity values than that of the secondary amine.
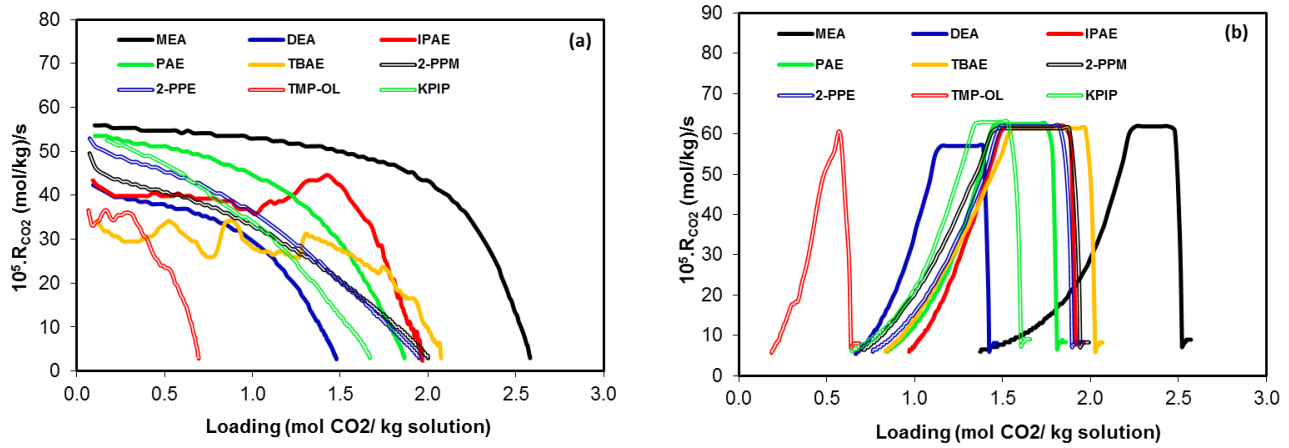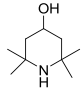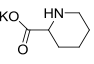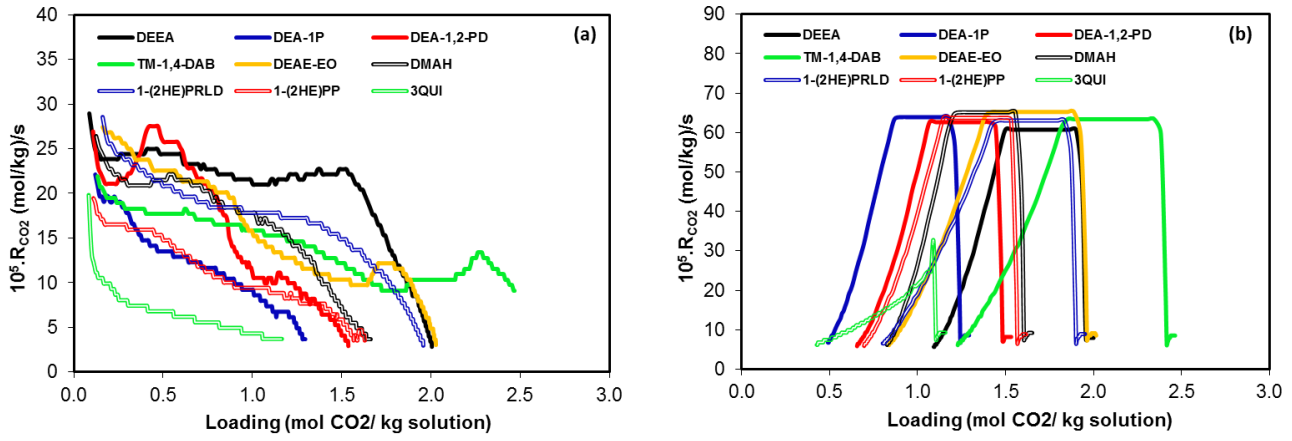

Figure 3. Absorption rate (a) and desorption rate (b) of secondary amine solvents as function of loading at 40°C and 80°C

Table 2. The absorption and desorption at process conditions for secondary amines

No	Solvent		Process	
	Name	Structure	Absorption	Desorption
1	IPAE		•Duration = 105.5 min •DEA~$R_{CO2}^{Abs.}$*<MEA •DEA<Rich loading<MEA •μ_{MEA}^{Rich}~$\mu_{DEA}^{Rich} < \mu_{IPAE}^{Rich}$ •$FI \gg DEA{\sim}MEA$	•Duration = 69.5 min •DEA~$R_{CO2}^{Des.}$**<MEA •DEA<Lean loading<MEA •$\mu_{MEA}^{Lean} < \mu_{DEA}^{Lean} < \mu_{IPAE}^{Lean}$ •$FI \gg DEA{\sim}MEA$
2	PAE		•Duration = 102.5 min •DEA<<$R_{CO2}^{Abs.}$*<MEA •DEA<Rich loading<MEA •μ_{MEA}^{Rich}~$\mu_{DEA}^{Rich} < \mu_{PAE}^{Rich}$ •$FI = DEA{\sim}MEA$	•Duration = 81.5 min •DEA~$R_{CO2}^{Des.}$**<MEA •DEA<Lean loading<MEA •$\mu_{MEA}^{Lean} < \mu_{DEA}^{Lean} < \mu_{PAE}^{Lean}$ •$FI = DEA{\sim}MEA$
3	tBAE		•Duration = 143.5 min •$R_{CO2}^{Abs.}$*<DEA<MEA •DEA<Rich loading<MEA •μ_{MEA}^{Rich}~$\mu_{DEA}^{Rich} < \mu_{tBAE}^{Rich}$ •$FI > DEA{\sim}MEA$	•Duration = 85.5 min •$R_{CO2}^{Des.}$**<DEA< MEA •DEA<Lean loading<MEA •$\mu_{MEA}^{Lean} < \mu_{DEA}^{Lean} < \mu_{tBAE}^{Lean}$ •$FI > DEA{\sim}MEA$
4	2-PPM		•Duration = 156.5 min •DEA<$R_{CO2}^{Abs.}$*<MEA •DEA<Rich loading<MEA •μ_{MEA}^{Rich}~$\mu_{DEA}^{Rich} < \mu_{2-PPM}^{Rich}$ •$FI = DEA{\sim}MEA$	•Duration = 93.5 min •$R_{CO2}^{Des.}$**<DEA< MEA •DEA~Lean loading<MEA •$\mu_{MEA}^{Lean} < \mu_{DEA}^{Lean} < \mu_{2-PPM}^{Lean}$ •$FI = DEA{\sim}MEA$
5	2-PPE		•Duration = 144.5 min •DEA<<$R_{CO2}^{Abs.}$*<MEA •DEA<Rich loading<MEA •μ_{MEA}^{Rich}~$\mu_{DEA}^{Rich} < \mu_{2-PPE}^{Rich}$ •$FI = DEA{\sim}MEA$	•Duration = 91.5 min •$R_{CO2}^{Des.}$**<DEA< MEA •DEA<Lean loading<MEA •$\mu_{MEA}^{Lean} < \mu_{DEA}^{Lean} < \mu_{2-PPE}^{Lean}$ •$FI = DEA{\sim}MEA$

| 6 | TMP-OL | | •Low concentration
•Duration = 50.5 min
•$R_{CO2}^{Abs.}$*<DEA<MEA
•Rich loading<DEA<MEA
•$\mu_{MEA}^{Rich} \sim \mu_{DEA}^{Rich} > \mu_{TMP-OL}^{Rich}$
•$FI > DEA \sim MEA$ | •Duration = 47.5 min
•$R_{CO2}^{Des.}$**<<DEA< MEA
•Lean loading<DEA< MEA
•$\mu_{MEA}^{Lean} < \mu_{DEA}^{Lean} < \mu_{TMP-OL}^{Lean}$
•$FI > DEA \sim MEA$ |
| 7 | KPIP | | •Duration = 112.5 min
•DEA<<$R_{CO2}^{Abs.}$*<MEA
•DEA<Rich loading< MEA
•$\mu_{MEA}^{Rich} \sim \mu_{DEA}^{Rich} \ll \mu_{KPIP}^{Rich}$
•$FI = DEA \sim MEA$ | •Duration = 90.5 min
•DEA~$R_{CO2}^{Des.}$**<MEA
•DEA~Lean loading<MEA
•$\mu_{MEA}^{Lean} < \mu_{DEA}^{Lean} < \mu_{KPIP}^{Lean}$
•$FI = DEA \sim MEA$ |

$*R_{CO2}^{Abs.} = R_{CO2}$ @lean loading $**R_{CO2}^{Des.} = R_{CO2}$ @rich loading
$\mu = viscocity \ (mPa.s)$ $FI = Foaminess\ coefficent\ (s)$

3.1.2. Tertiary amines

Eight different tertiary amine solvent candidates (5 linear carbons and 3 cyclic carbons) were tested in this work. The results can been seen in Figure 4 and summarized in Table 3. The measured viscosities of both rich and loadings were also reported in Table A.3 (see Appendix A.3). Only TM-1,4-DAB has significant higher viscosities than that of MEA. During absorption process, 6 solvent candidates (DEA-1P, DEA-1,2-PD, TM-1,4-DAB, DEAE-EO, 1-(2HE)PP and DMAH) showed severe foaming tendency and the foaminess coefficient showed higher value than that of MEA (see in Appendix A.4). Both 1-(2HE)PRLD and 3QUI solvents had foaming tendencies similar to that of MEA.

For all solvents, the initial absorption rates as well as rich loading are lower than those of DEEA. TM-1,4-DAB reached higher rich loading than DEEA, but this is most likely due to enhancement caused by the foam. No precipitation and no discoloration were observed. During desorption process, all solvents except TM-1,4-DAB gave lower lean loading than that of DEEA. 3QUI solvent shows low desorption rate.
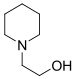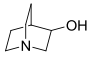
Figure 4. Absorption rate (a) and desorption rate (b) of secondary amine solvents as function of loading at 40°C and 80°C

Table 3. The absorption and desorption at process conditions for tertiary amines

No	Solvent		Process	
			Absorption	Desorption
1	DEA-1P		• Duration = 195.5 min • $R_{CO2}^{Abs.}*<DEEA<<<$ MEA • DEEA<Rich loading<MEA • $\mu_{MEA}^{Rich} < \mu_{DEA-1P}^{Rich} < \mu_{DEEA}^{Rich}$ • $FI > DEEA > MEA$	• Duration = 54.5 min • DEEA$<R_{CO2}^{Des.}**<$MEA • Lean loading<DEEA<MEA • $\mu_{MEA}^{Lean} < \mu_{DEA-1P}^{Lean} \sim \mu_{DEEA}^{Lean}$ • $FI \sim DEEA > MEA$
2	DEA-1,2-PD		• Duration = 195.5 min • DEEA$\sim R_{CO2}^{Abs.}*<<<$MEA • DEEA<Rich loading<MEA • $\mu_{MEA}^{Rich} < \mu_{DEEA}^{Rich} < \mu_{DEA-1,2-PD}^{Rich}$ • $FI > DEEA > MEA$	• Duration = 59.5 min • DEEA$<R_{CO2}^{Des.}**<$MEA • Lean loading<DEEA<MEA • $\mu_{MEA}^{Lean} < \mu_{DEEA}^{Lean} < \mu_{DEA-1,2-PD}^{Lean}$ • $FI > DEEA > MEA$
3	TM-1,4-DAB		• Duration = 299.5 min • $R_{CO2}^{Abs.}*<DEEA<<<$ MEA • DEEA<Rich loading~MEA • $\mu_{MEA}^{Rich} < \mu_{DEEA}^{Rich} < \mu_{TM-1,4-DAB}^{Rich}$ • $FI > DEEA > MEA$	• Duration = 78.5 min • $R_{CO2}^{Des.}**<DEEA<$MEA • DEEA<Lean loading~MEA • $\mu_{MEA}^{Lean} < \mu_{DEEA}^{Lean} < \mu_{TM-1,4-DAB}^{Lean}$ • $FI > DEEA > MEA$
4	DEAE-EO		• Duration = 236.5 min • DEA$\sim R_{CO2}^{Abs.}*<<<$MEA • DEEA~Rich loading<MEA • $\mu_{MEA}^{Rich} < \mu_{DEEA}^{Rich} < \mu_{DEAE-EO}^{Rich}$ • $FI > DEEA > MEA$	• Duration = 71.5 min • DEEA$\sim R_{CO2}^{Des.}**<$MEA • Lean loading<DEEA<MEA • $\mu_{MEA}^{Lean} < \mu_{DEEA}^{Lean} < \mu_{DEAE-EO}^{Lean}$ • $FI > DEEA > MEA$
5	DMAH		• Duration = 196.5 min • DEEA$\sim R_{CO2}^{Abs.}*<<<$MEA • DEEA<Rich loading<MEA • $\mu_{MEA}^{Rich} < \mu_{DEEA}^{Rich} < \mu_{DMAH}^{Rich}$ • $FI > DEEA > MEA$	• Duration = 53.5 min • DEEA$<R_{CO2}^{Des.}**<$MEA • Lean loading<DEEA<MEA • $\mu_{MEA}^{Lean} < \mu_{DEEA}^{Lean} < \mu_{DMAH}^{Lean}$ • $FI > DEEA > MEA$
6	1-(2HE)PRLD		• Duration = 209.5 min • DEEA$\sim R_{CO2}^{Abs.}*<$MEA • DEEA~Rich loading<MEA • $\mu_{MEA}^{Rich} < \mu_{1-(2HE)PRLD}^{Rich} < \mu_{DEEA}^{Rich}$ • $DEEA > FI = MEA$	• Duration = 76.5 min • DEA$\sim R_{CO2}^{Des.}**<$MEA • Lean loading<DEEA<MEA • $\mu_{MEA}^{Lean} < \mu_{1-(2HE)PRLD}^{Lean} \sim \mu_{DEEA}^{Lean}$ • $DEEA > FI = MEA$

7	1-(2HE)PP		• Duration = 271.5 min • $R_{CO2}^{Abs.}$*<DEEA<<<MEA • DEEA<Rich loading<MEA • $\mu_{MEA}^{Rich} < \mu_{1-(2HE)PP}^{Rich} < \mu_{DEEA}^{Rich}$ • $FI = DEEA > MEA$	• Duration = 61.5 min • DEEA<$R_{CO2}^{Des.}$**<MEA • Lean loading<DEEA<MEA • $\mu_{MEA}^{Lean} < \mu_{1-(2HE)PP}^{Lean} < \mu_{DEEA}^{Lean}$ • $FI = DEEA > MEA$
8	3QUI		• Duration = 311.5 min • $R_{CO2}^{Abs.}$*<<DEEA<<<MEA • Rich loading<<DEEA< MEA • More than 5 hours operation • $\mu_{MEA}^{Rich} < \mu_{DEEA}^{Rich} < \mu_{3QUI}^{Rich}$ • $DEEA > FI = MEA$	• Duration = 102.5 min • $R_{CO2}^{Des.}$**<<DEEA<MEA • Lean loading<DEEA<MEA • $\mu_{MEA}^{Lean} < \mu_{DEEA}^{Lean} < \mu_{3QUI}^{Lean}$ • $DEEA > FI = MEA$
*$R_{CO2}^{Abs.} = R_{CO2}$ @lean loading μ = viscocity (mPa.s)			**$R_{CO2}^{Des.} = R_{CO2}$ @rich loading $FI = Foaminess\ coefficent\ (s)$	

3.1.3. Screening Performance of the solvent candidates

For Figure 5, it is seen that the rich loadings of most the solvent was lower compared to MEA. Only TM-1,4-DAB has rich loading comparable to MEA. All solvents have lower lean loading after the stripping process compared to MEA. This indicates that the solvents have good potential of releasing CO_2 during the desorption process.
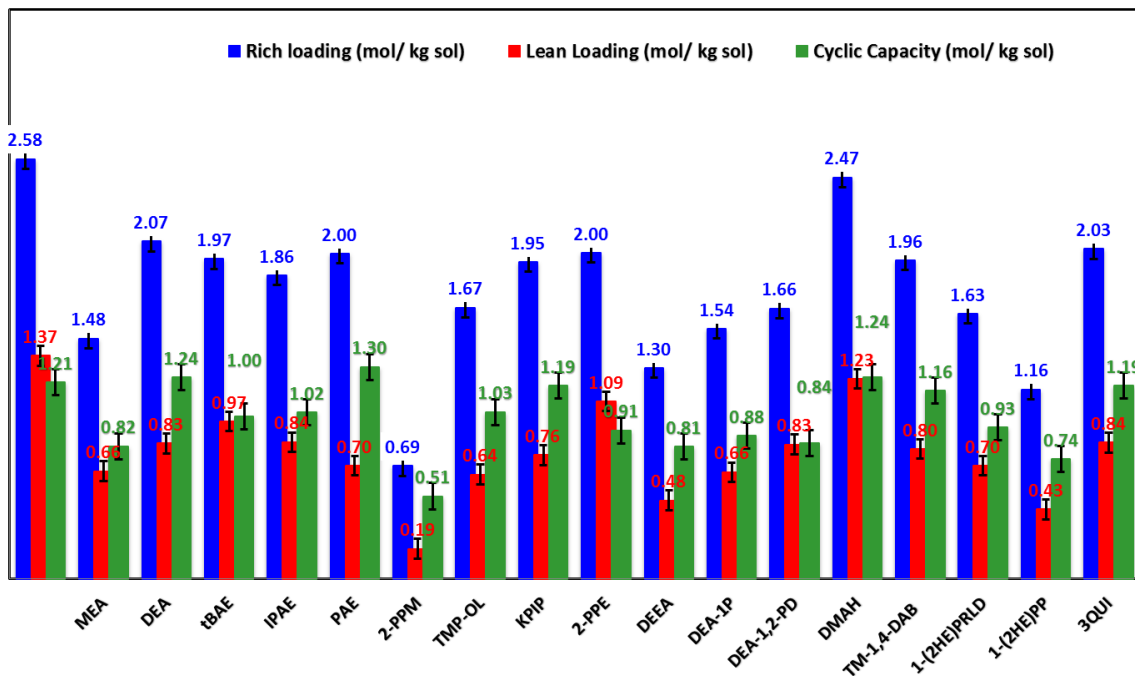
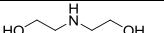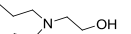**Figure 5. Screening performance of solvent candidates**
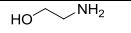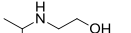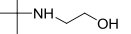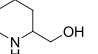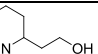
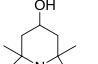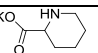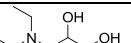The cyclic capacity was estimated from the rich and lean loadings (see Eq. 4). Only one solvent candidate (2-PPM) showed clearly higher cyclic capacity than MEA while tBAE, 2-PPE, TM-1,4-DAB,
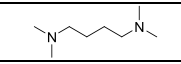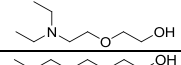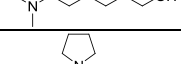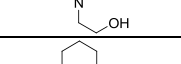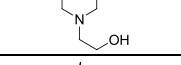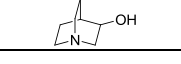
1-(2HE)PRLD and DEEAE-EO have cyclic capacity comparable to MEA. From these solvent candidates tBAE, TM-1,4-DAB and DEEAE-EO has foaming issue. Furthermore, 2-PPM has high melting point (~70°C) that may become an issue (solidification) in plant operation during shutdowns.

3.2. Dissociation constant (pKa)

pKa values was used as one of the factors for solvent recommendations. To confirm the literature values and to measure pKa for those solvent candidates for which pKa values were not available, the dissociation constants of all tested solvent candidates were measured at very low concentration ~0.01m (assuming as an infinite solution) and at 25°C. The results along with available data are collected in Table 4. For MEA, DEA, DEEA and 1-(2HE)PRLD the results agree well with literature. Some disagreements were seen between our data and the reported data in literature. This is because different experiment conditions used i.e. temperature (23 to 26°C) and (unspecified) solvent concentration. It is known that if higher concentrations are used, the initial pH and pKa values become higher.

Table 4. Measured pKa values (uncertainty±0.02) at 0.01 m and at 25 ºC (NA = Not Available).

No	Solvent		pKa value	
	Name	Structure	This work	Literature(s)
R1	MEA		9.50	9.44(Hamborg and Versteeg, 2009) 9.508(Kim et al., 1987)
R2	DEA		8.92	8.88(Vincent E. Bower, 1962)
R3	DEEA		9.75	9.75(Hamborg and Versteeg, 2009) 10.01(Chowdhury et al., 2013a)
1	IPAE		9.78	NA
2	PAE		9.89	9.90(Perrin, 1965)
3	tBAE		10.04	NA
4	2-PPM		10.12	NA
5	2-PPE		10.42	10.14(Xu et al., 1992) 10.48(Fernandes et al., 2012)
6	TMP-OL		9.99	10.05 (Perrin, 1965)
7	KPIP		10.50	NA
8	DEA-1P		9.67	10.29(Chowdhury et al., 2013a)
9	DEA-1,2-PD		9.68	9.89(Chowdhury et al., 2013a)

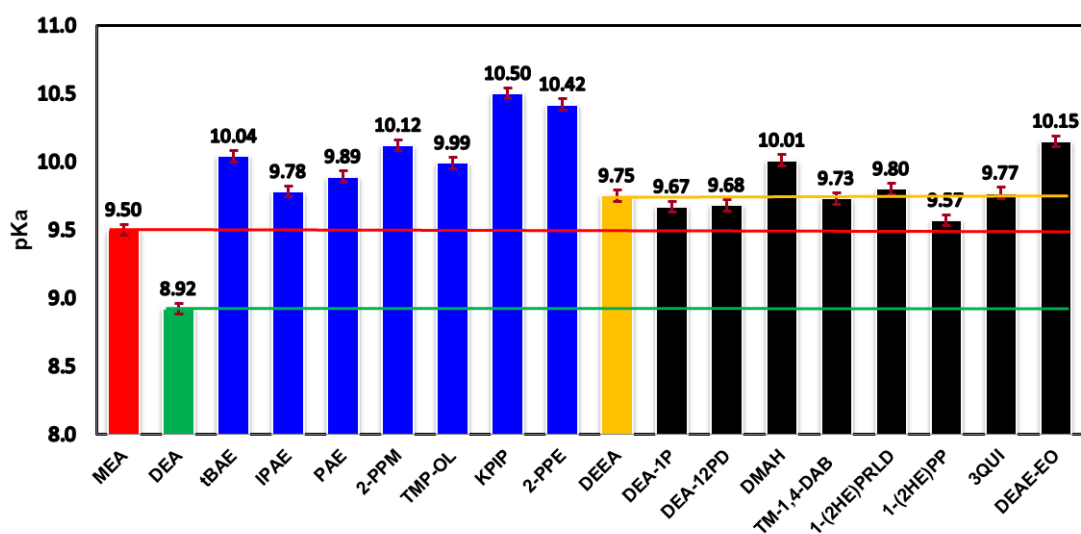| 10	TM-1,4-DAB		9.73	NA
11	DEAE-EO		10.15	NA
12	DMAH		10.01	NA
13	1-(2HE)PRLD		9.80	9.86(Chowdhury et al., 2013a)
14	1-(2HE)PP		9.57	9.76(Chowdhury et al., 2013a)
15	3QUI		9.77	NA

Figure 6. pKa values (at ~0.01 m, 25°C) for different solvent candidates (blue bars, secondary amines; black bars, tertiary amines; red line, pKa of MEA; green line, pKa of DEA; yellow line, pKa of DEEA)

All solvent candidates have higher pKa value than that of MEA and DEA but only seven solvents showed significant higher pKa values than that of DEEA (pKa $\geq$ 9.99). Eight solvents showed comparable value to that of DEEA (pKa = 9.57 to 9.89) (see in Figure 6). 2-PPE shows clearly higher pKa compared to the reference solvents, whereas the other solvent chosen for characterization, 1-(2HE)PRLD, has pKa values similar to DEEA.

High pKa value is expected to give fast absorption rate. Therefore, the absorption rate and the cyclic capacity from the screening experiments were plotted as a function of pKa. From Figure 7, we can see

that 2-PPE shows high absorption capacity and can be found in the upper right corner in Figure 7(a) whereas 1-(2HE)PRLD with lower pKa had much lower absorption rate and can therefore be found in the middle of the figure together with the other tertiary amines. Based on this figure, PAE shows somewhat unexpectedly high absorption rate. Furthermore, based purely on this figure KPIP, PAE and 2-PPE are showing good performance. However KPIP was not considered to be a promising solvent due to low cyclic capacity (less than that of MEA), as shown in Figure 5, a possible solid formation at higher loadings and concentrations as well as due to its high carbamate to bicarbonate ratio making it not very strong bicarbonate former. While PAE has low cyclic capacity making it not suitable, see Figure 5. In Figure 7(b) the cyclic capacities are plotted as a function of pKa. As already discussed previously tBAE, 2-PPM, 2-PPE, TM-1,4-DAB, 1-(2HE)PRLD and DEEAE-EO have cyclic capacity comparable to MEA. In consideration to foaming tendencies and high melting point most of these solvents were not taken for further studies and only 2-PPE and 1-(2HE)PRLD were chosen for further characterization.

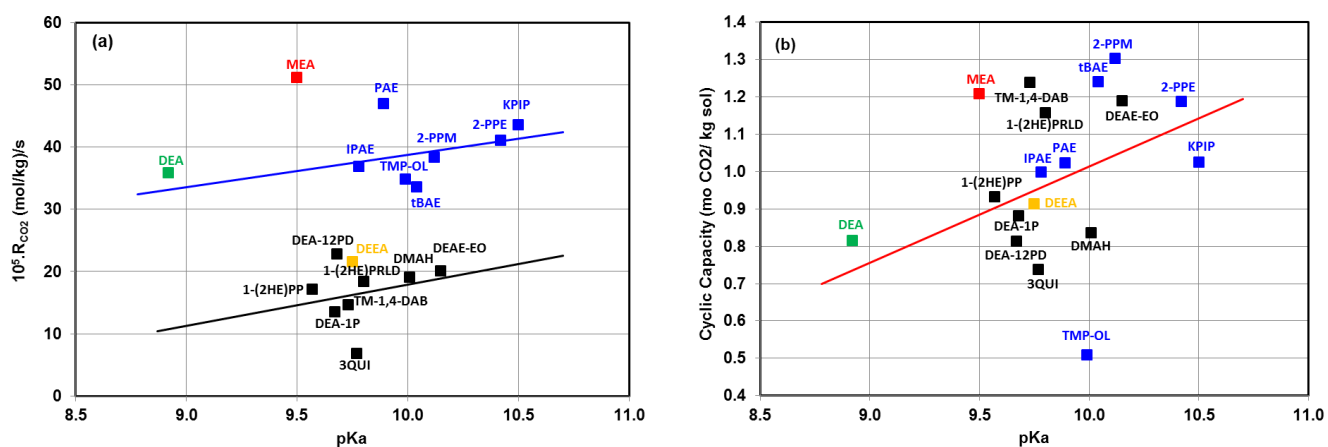**Figure 7. Absorption rate at 40°C (a) and cyclic capacity (b) as a function of pKa value (■, Secondary amines, ■; tertiary amines; solid lines, trend lines)**

3.3. Further characterization

Further optimization of the chosen solvents was pursued through variation of the concentration using the screening apparatus. Four different concentrations (30 to 60 mass% of solvent) were tested and the

results are shown in Figure 8 for 2-PPE and in Figure 10 for 1-(2HE)PRLD. Viscosities both rich and lean loadings were measured and reported in Figure A.3.1. (See Appendix A.3). The viscosity increases with increasing concentration for both systems.

Initial absorption rate of 2-PPE solutions were faster than that of DEA but lower than that of MEA. The initial absorption rates at 50 and 60 mass% aqueous solutions of 2-PPE are slightly lower than those of 30 and 40 mass% aqueous solutions as increased viscosity. However, at the same time the 50 and 60 mass% solutions showed higher rich loadings compared to 30 mass% MEA. No foaming tendencies nor formation of solids was observed in the experiment. During the desorption process, 30 mass% 2-PPE showed lowest lean loading. Additionally the lean loading of 50 and 60 mass% 2-PPE was almost the same and similar to that of DEEA. As a summary of the results it can be concluded that the both the rich loading and lean loading increased with concentration from 30 to 50 mass% as shown in Figure 9(a). No further improvement was seen with 60 mass % solution. The maximum cyclic capacity (~1.77 mol CO_2/ kg solvent) is seen at 50 mass% solution. The cyclic capacity of 50 mass% 2-PPE is almost 50% higher compared to 30 mass% MEA (~1.21 mol CO_2/ kg solvent).
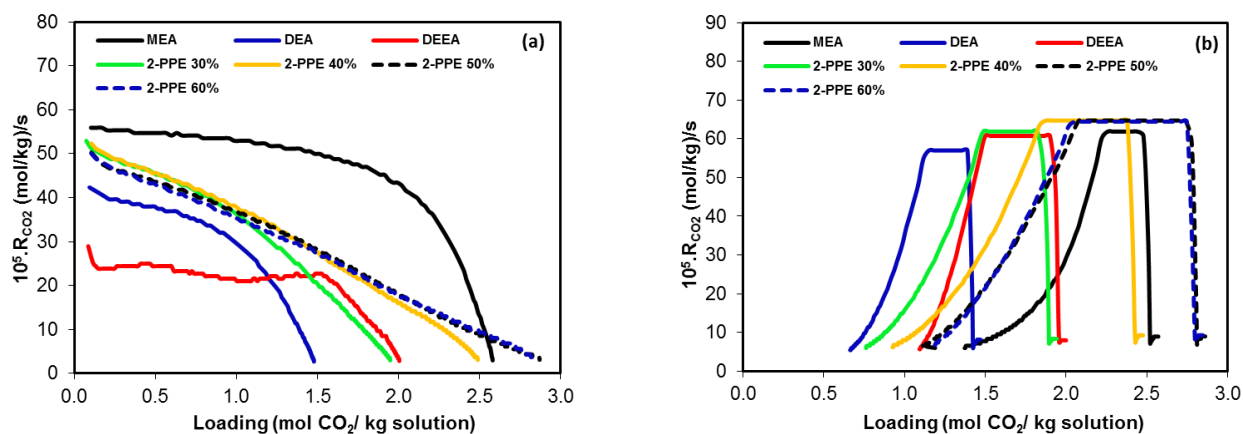

Figure 8. Absorption rate (a) and desorption rate (b) of 2-PPE solvents as function of loading at 40°C and 80°C
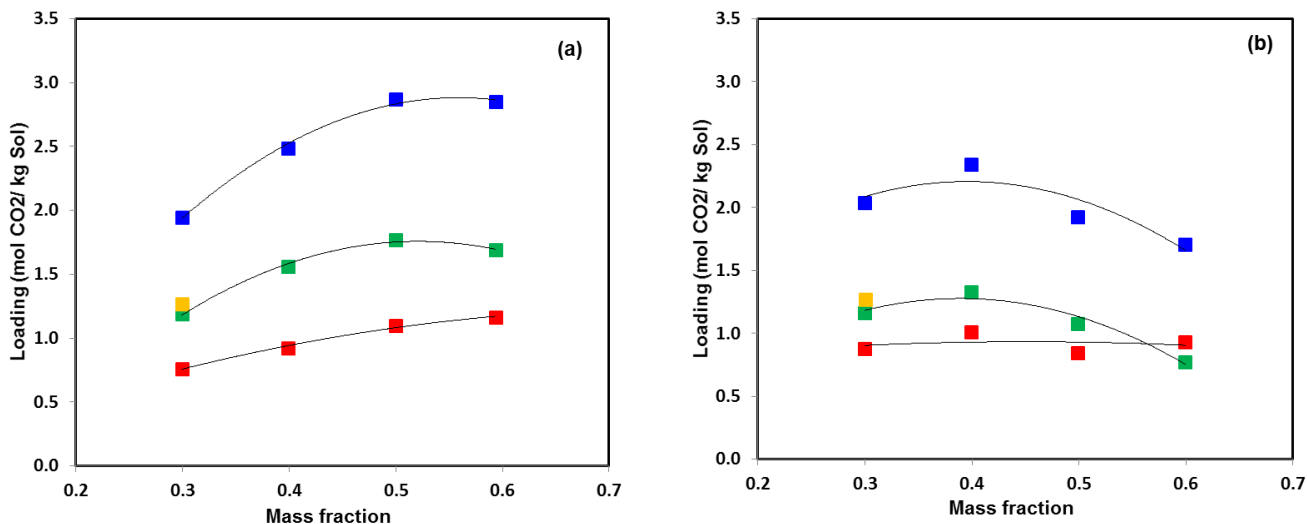
Figure 9. Screening performances of (a) 2-PPE (b) 1-(2HE)PRLD solvents at different concentrations (■, rich loading; ■, lean loading; ■, cyclic capacity; ■, cyclic capacity of 30 mass % MEA; Solid lines, trend lines).

1-(2HE)PRLD showed lower initial absorption rates than the tertiary amine DEEA and 2-PPE. The initial absorption rate of 30 mass% aqueous 1-(2HE)PRLD was faster than at higher concentrations due to increasing viscosity (see Appendix A3, Figure A3.1) . For all tested concentrations, the rich loadings were lower than that of 30 mass % of MEA. No solid formations were observed in the experiment. However foaming tendencies was observed during the testing of 30 and 40 mass% 1-(2HE)PRLD as seen in Figure 10a. Overall, the lean loading was independent to concentration studied, but rich loading reach maximum at 40 mass% then decreased at higher concentration as seen from Figure 9b. Thus the highest cyclic capacity was found with 40 mass% of 1-(2HE)PRLD (~1.33 mol CO_2/ kg solvent).
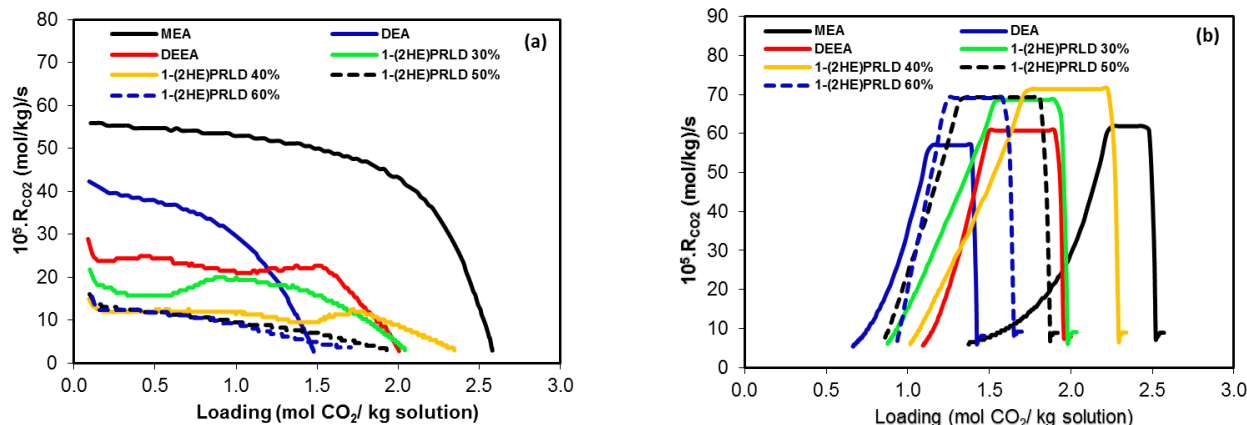
Figure 10. Absorption rate (a) and desorption rate of (b) of 1-(2HE)PRLD solvents as function of loading at 40°C and 80°C.

4. Conclusion

Fifteen solvent candidates were tested in the screening apparatus where an absorption and a desorption process in CO_2 capture plant were mimicked. Absorption was done at 40◦C until 95% ofthe CO2was captured while desorption process was done at 80◦Cand 90% CO2removal. The solvent performance (rich/lean loadingand cyclic capacity) were compared with the reference solvents(MEA, DEA and DEEA).. In addition, solvent appearances, such assolid formation, foaming tendency and viscosity change, duringthe process were also reported. Viscosities of rich and lean load-ings were measured and the foaming tendencies were estimated.No solid formation nor viscosity issue were observed. However,several solvent candidates were foaming during the experiments.

The screening results show that six solvent candidates havecomparable cyclic capacity to MEA, i.e three secondary amines sol-vents (tBAE, 2-PPM and 2-PPE) and three tertiary amine solvents(TM-1,4-DAB, 1-2(HE)PRLD and DEAE-EO). Three solvents (tBAE,TM-1,4-DAB and DEAE-EO) were observed have foaming tendency.2-PPM has the highest cyclic capacity.

Dissociation constants were measured at low concentration(0.01 m) and at 25◦C. It was observed that the pKa values are largerthan that of MEA. Together with screening result, it is seen thatcyclic capacity and the absorption rate increase with the pKa value.

Based on the screening and pKa measurements, two solvents (2-PPE and 1-2(HE)PRLD) were selected to further studies to find theoptimum concentration with maximum cyclic capacity. The highestcyclic capacities were reached with 50 mass% 2-PPE and with 40mass% 1-(2HE)PRLD showing 50% and 10% higher cyclic capacitiescompared to MEA, respectively.

ACKNOWLEDGMENT

APPENDIX

A1. Screening Procedure verification

The screening apparatus was verified with a benchmarking solvent MEA 30 mass%. The initial concentration of CO_2 gas inlet was set to 10% (10 kPa). The absorption was done at 40°C and at 95% absorption (CO_2 outlet = 9.5% /9.5 kPa). The desorption process was done at 80°C and it was stopped at 90% removal (CO_2 outlet = 1.0%/ 1.0 kPa). The sample was taken after both absorption and desorption processes and titrated for amine and CO_2 concentrations (Ma'mun et al., 2006). The result is showed in Table A1, together with the reported VLE data/ model (Aronu et al., 2011a). As it might be seen that the CO_2 content estimated from the gas phase (Equation 5), liquid analysis and VLE data are in good agreement. The difference between the liquid titration and results based on gas phase (Equation 5) can be used to get an idea of the overall uncertainty in the experiments. In this case the average difference is 4.9%.

Table A1. Verification for the screening procedure.

Sample	P_{CO_2} (kPa)	T (°C)	Loading						Remark
			Equation 5		Titration		VLE		
			$\left(\frac{mol\ CO2}{kg\ Sol}\right)$	$\left(\frac{mol\ CO2}{mol\ MEA}\right)$	$\left(\frac{mol\ CO2}{kg\ Sol}\right)$	$\left(\frac{mol\ CO2}{mol\ MEA}\right)$	$\left(\frac{mol\ CO2}{kg\ Sol}\right)$	$\left(\frac{mol\ CO2}{mol\ MEA}\right)$	
Absorption	9.5	40	2.58	0.53	2.77	0.55	2.61	0.52	Rich Loading
Desorption	1.0	80	1.37	0.28	1.33	0.25	1.27	0.26	Lean Loading

A.2. Estimated uncertainty

Uncertainties of CO_2 absorbed $\left(Q_{CO_2}\right)$, Accumulated CO_2 $\left(N_{CO_2}\right)$, rate of absorption/ desorption $\left(r_{CO_2}\right)$, Cyclic capacity $\left(Q_{cyc}\right)$, loading (α) (Equations 1-5) were estimated by Gaussian's error propagation (Ellison, 2012) according to :

$$s_y^2 \approx \Sigma_i^N \left(\frac{\partial y}{\partial x_i}\right)^2 \cdot s_x^2 \tag{A2.1}$$

$$U(S_Y) = \pm \sqrt[2]{\Sigma_i^N \left(\frac{\partial y}{\partial x_i}\right)^2 \cdot s_x^2} \tag{A2.2}$$

By taking first derivation of equation 1 to 5 with respect to independent variables and then including the standard uncertainties of its variables (MFC of N_2, MFC of CO_2, CO_2 analyzer and the scale), the estimated combined uncertainties are showed in Table A.2. The values are expected to be constant since they were calculated using a coverage factor by 2 to give a 95% level of confidence.

Table A.2. Estimated combined uncertainties

Source	$U(S_Y)$
$Q_{CO_2} \left(\frac{mol\ CO2}{s}\right)$	$\pm 1 \cdot 10^{-5}$
$r_{CO_2} \left(\frac{mol\ CO2}{kg\ sol \cdot s}\right)$	$\pm 2 \cdot 10^{-6}$
$N_{CO_2} (mol\ CO2)$	$\pm 7 \cdot 10^{-4}$
$\alpha \left(\frac{mol\ CO2}{kg\ sol}\right)$	$\pm 6 \cdot 10^{-3}$
$Q_{cyc} \left(\frac{mol\ CO2}{kg\ sol}\right)$	$\pm 8 \cdot 10^{-3}$

A.3. Measured Viscosity

Viscosities of both rich and lean loadings were measured in Rheometer MCR 100 at 25°C. The detail procedure can be found in Hartono et al. (2014b).
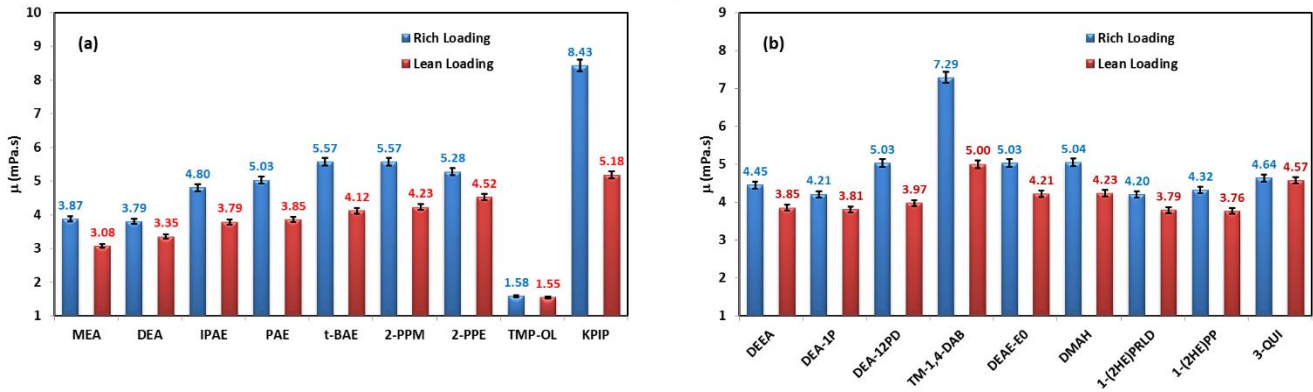

Figure A3. Viscosities of rich and lean loadings at 25°C for solvent candidates of (a) secondary amine (b) tertiary amines.
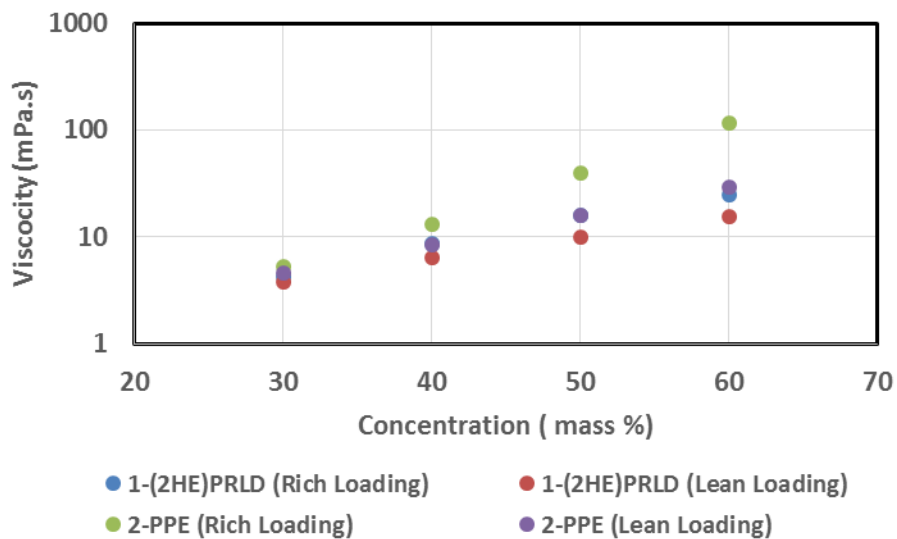

Figure A3.1. Measured viscosity of the selected system both rich and lean loadings at 25°C

A.4. Estimated foaminess coefficient (FI).

Foaminess coefficient (Thitakamol and Veawab, 2008) was directly measured in the experimental condition (40°C/ 80°C and N2 = ~0.9 NL/min). Comparing the numbers to MEA show an information how challenge would be for the new system. If the value is higher than that of MEA then it indicates a potential foaming tendency. An anti-foaming agent might be needed when the coefficient showed much higher than that of MEA. At desorption condition, the observed foaming tendency slightly reduce due to increasing temperature as expected.
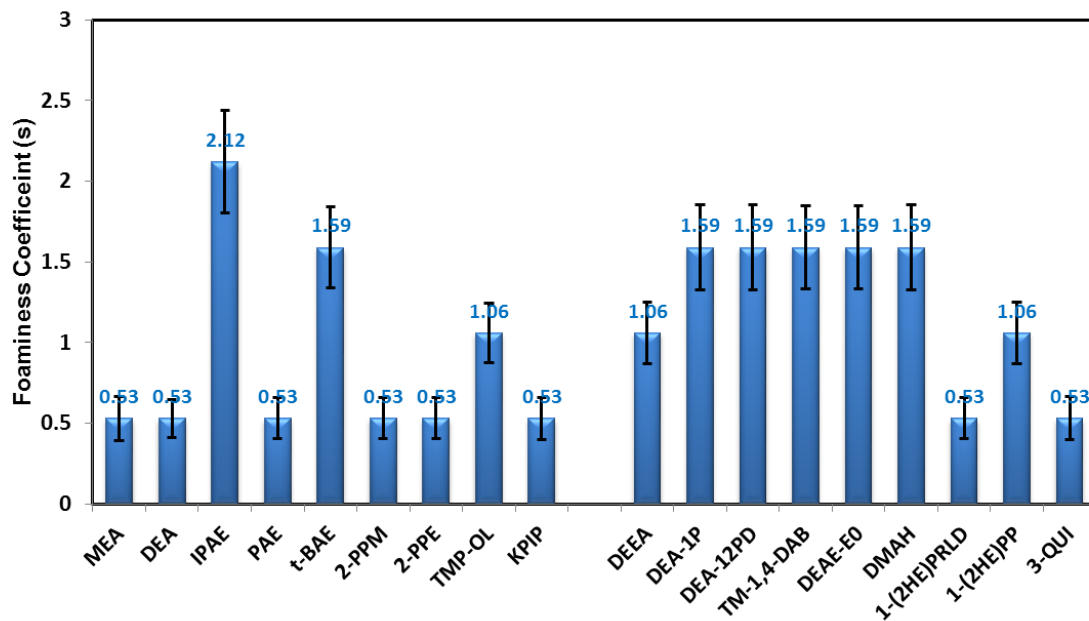

Figure A4. Estimated foaminess Coefficient (s) of different solvent at absorption condition (40°C and N$_2$ = ~0.9 NL/min)

REFERENCES

Aronu, U.E., Gondal, S., Hessen, E.T., Haug-Warberg, T., Hartono, A., Hoff, K.A., Svendsen, H.F., 2011a. Solubility of CO2 in 15, 30, 45 and 60 mass% MEA from 40 to 120°C and model representation using the extended UNIQUAC framework. Chemical Engineering Science 66, 6393-6406.

Aronu, U.E., Hoff, K.A., Svendsen, H.F., 2011b. CO2 capture solvent selection by combined absorption-desorption analysis. Chemical Engineering Research and Design 89, 1197-1203.

Aronu, U.E., Svendsen, H.F., Hoff, K.A., 2010. Investigation of amine amino acid salts for carbon dioxide absorption. International Journal of Greenhouse Gas Control 4, 771-775.

Bonenfant, D., Mimeault, M., Hausler, R., 2003. Determination of the Structural Features of Distinct Amines Important for the Absorption of CO2 and Regeneration in Aqueous Solution. Industrial & Engineering Chemistry Research 42, 3179-3184.

Bouchoux, G., 2007. Gas-phase basicities of polyfunctional molecules. Part 1: theory and methods. Mass Spectrom. Rev. 26, 775-835.

Brúder, P., Grimstvedt, A., Mejdell, T., Svendsen, H.F., 2011. CO2 capture into aqueous solutions of piperazine activated 2-amino-2-methyl-1-propanol. Chemical Engineering Science 66, 6193-6198.

Caplow, M., 1968. Kinetics of carbamate formation and breakdown. J. Amer. Chem. Soc. 90, 6795-6803.

Carey, F.A., Sundberg, R.J., 2000. Advanced Organic Chemistry. Part A: Structure and Mechanisms, 4 ed. Kluwer Academic/Plenum Publishers, New York, Boston, Dirdrecht, London, Moscow.

Chakraborty, A.K., Astarita, G., Bischoff, K.B., 1986. CO2 absorption in aqueous solutions of hindered amines. Chemical Engineering Science 41, 997-1003.

Chakraborty, A.K., Bischoff, K.B., Astarita, G., Damewood, J.R., Jr., 1988. Molecular orbital approach to substituent effects in amine-CO2 interactions. J. Am. Chem. Soc. 110, 6947-6954.

Chen, E., Madan, T., Sachde, D., Walters, M.S., Nielsen, P., Rochelle, G.T., 2013. Pilot Plant Results with Piperazine. Energy Procedia 37, 1572-1583.

Chowdhury, F.A., Okabe, H., Shimizu, S., Onoda, M., Fujioka, Y., 2009. Development of novel tertiary amine absorbents for CO2 capture. Energy Procedia 1, 1241-1248.

Chowdhury, F.A., Okabe, H., Yamada, H., Onoda, M., Fujioka, Y., 2011. Synthesis and selection of hindered new amine absorbents for CO2 capture. Energy Procedia 4, 201-208.

Chowdhury, F.A., Yamada, H., Higashii, T., Goto, K., Onoda, M., 2013a. CO2 Capture by Tertiary Amine Absorbents: A Performance Comparison Study. Industrial & Engineering Chemistry Research 52, 8323-8331.

Chowdhury, F.A., Yamada, H., Higashii, T., Matsuzaki, Y., Kazama, S., 2013b. Synthesis and characterization of new absorbents for CO2 capture. Energy Procedia 37, 265-272.

Ciftja, A.F., Hartono, A., Svendsen, H.F., 2014. Amine neutralized amino acid as CO2 absorbents: A quantitative 13C-NMR study. International Journal of Greenhouse Gas Control 27, 169-177.

da Silva, E.F., 2005. Comparison of Quantum Mechanical and Experimental Gas-Phase Basicities of Amines and Alcohols. J. Phys. Chem. A 109, 1603-1607.

da Silva, E.F., 2011. Theoretical study of the equilibrium constants for solvents for CO2 capture. Energy Procedia 4, 164-170.

da Silva, E.F., Svendsen, H.F., 2003. Prediction of the pKa Values of Amines Using ab Initio Methods and Free-Energy Perturbations. Ind. Eng. Chem. Res. 42, 4414-4421.

da Silva, E.F., Svendsen, H.F., 2006. Study of the Carbamate Stability of Amines Using ab Initio Methods and Free-Energy Perturbations. Ind. Eng. Chem. Res. 45, 2497-2504.

da Silva, E.F., Svendsen, H.F., 2007. Computational chemistry study of reactions, equilibrium and kinetics of chemical CO2 absorption. Int. J. Greenhouse Gas Control 1, 151-157.

Ellison, S.L.R.a.W.A., 2012. Eurachem/CITAC guide: Quantifying Uncertainty in Analytical Measurement.

Ewing, S.P., Lockshon, D., Jencks, W.P., 1980. Mechanism of cleavage of carbamate anions. J. Am. Chem. Soc. 102, 3072-3084.

Fernandes, D., Conway, W., Wang, X.G., Burns, R., Lawrance, G., Maeder, M., Puxty, G., 2012. Protonation constants and thermodynamic properties of amines for post combustion capture of CO2. Journal of Chemical Thermodynamics 51, 97-102.

Freeman, S.A., Dugas, R., Van Wagener, D.H., Nguyen, T., Rochelle, G.T., 2010. Carbon dioxide capture with concentrated, aqueous piperazine. International Journal of Greenhouse Gas Control 4, 119-124.

Goto, K., Chowdhury, F.A., Okabe, H., Shimizu, S., Fujioka, Y., 2011a. Development of a low cost CO2 capture system with a novel absorbent under the COCS project. Energy Procedia 4, 253-258.

Goto, K., Okabe, H., Chowdhury, F.A., Shimizu, S., Fujioka, Y., Onoda, M., 2011b. Development of novel absorbents for CO2 capture from blast furnace gas. Int. J. Greenhouse Gas Control 5, 1214-1219.

Gupta, M., da Silva, E.F., Svendsen, H.F., 2012. Modeling Temperature Dependency of Amine Basicity Using PCM and SM8T Implicit Solvation Models. J. Phys. Chem. B 116, 1865-1875.

Hamborg, E.S., Versteeg, G.F., 2009. Dissociation Constants and Thermodynamic Properties of Amines and Alkanolamines from (293 to 353) K. Journal of Chemical & Engineering Data 54, 1318-1328.

Hartono, A., Ciftja, A.F., Brúder, P., Svendsen, H.F., 2014a. Characterization of amine-impregnated adsorbent for CCS post combustion, Energy Procedia, pp. 2138-2143.

Hartono, A., Mba, E.O., Svendsen, H.F., 2014b. Physical properties of partially CO2 loaded aqueous monoethanolamine (MEA). Journal of Chemical and Engineering Data 59, 1808-1816.

Hartono, A., Saeed, M., Kim, I., Svendsen, H.F., 2014c. Protonation Constant (pKa) of MDEA in Water as Function of Temperature and Ionic Strength. Energy Procedia 63, 1122-1128.

Hook, R.J., 1997. An Investigation of Some Sterically Hindered Amines as Potential Carbon Dioxide Scrubbing Compounds. Ind. Eng. Chem. Res. 36, 1779-1790.

Jackson, P., Beste, A., Attalla, M., 2011. Insights into amine-based CO2 capture: an ab initio self-consistent reaction field investigation. Struct Chem 22, 537-549.

Karpas, Z., 1992. The mobility of protonated amino alcohols: evidence for proton-induced cyclization. Struct. Chem. 3, 139-141.

Kim, I., Jens, C.M., Grimstvedt, A., Svendsen, H.F., 2011. Thermodynamics of protonation of amines in aqueous solutions at elevated temperatures. The Journal of Chemical Thermodynamics 43, 1754-1762.

Kim, J.H., Dobrogowska, C., Hepler, L.G., 1987. Thermodynamics of Ionization of Aqueous Alkanolamines. Can J Chem 65, 1726-1728.

Kohl, A.L., Nielsen, R.B., 1997. Gas purification, 5 ed.

Leo, A.J., 1991. [25] Hydrophobic parameter: Measurement and calculation, Methods in Enzymology. Academic Press, pp. 544-591.

Ma'mun, S., Jakobsen, J.P., Svendsen, H.F., Juliussen, O., 2006. Experimental and Modeling Study of the Solubility of Carbon Dioxide in Aqueous 30 Mass % 2-((2-Aminoethyl)amino)ethanol Solution. Industrial & Engineering Chemistry Research 45, 2505-2512.

Ma'mun, S., Svendsen, H.F., Hoff, K.A., Juliussen, O., 2007. Selection of new absorbents for carbon dioxide capture. Energy Conversion and Management 48, 251-258.

McCann, N., Phan, D., Fernandes, D., Maeder, M., 2011. A systematic investigation of carbamate stability constants by 1H NMR. Int. J. Greenhouse Gas Control 5, 396-400.

Mergler, Y., Gurp, R.R.-v., Brasser, P., Koning, M.d., Goetheer, E., 2011. Solvents for CO_2 capture. Structure-activity relationships combined with vapour-liquid-equilibrium measurements. Energy Procedia 4, 259-266.

Nielsen, P.T., Li, L., Rochelle, G.T., 2013. Piperazine Degradation in Pilot Plants. Energy Procedia 37, 1912-1923.

Perrin, D.D., 1965. Dissociation Constants of Organic Bases in aqueous solution, London.

Puxty, G., Rowland, R., Allport, A., Yang, Q., Bown, M., Burns, R., Maeder, M., Attalla, M., 2009. Carbon Dioxide Postcombustion Capture: A Novel Screening Study of the Carbon Dioxide Absorption Performance of 76 Amines. Environmental Science & Technology 43, 6427-6433.

Robinson, K., McCluskey, A., Attalla, M.I., 2012. The Effect Molecular Structural Variations Has on the CO_2 Absorption Characteristics of Heterocyclic Amines, Recent Advances in Post-Combustion CO_2 Capture Chemistry. American Chemical Society, pp. 1-27.

Sartori, G., Savage, D.W., 1983. Sterically hindered amines for carbon dioxide removal from gases. Industrial & Engineering Chemistry Fundamentals 22, 239-249.

Singh, P., Niederer, J.P.M., Versteeg, G.F., 2007. Structure and activity relationships for amine based CO2 absorbents—I. International Journal of Greenhouse Gas Control 1, 5-10.

Singh, P., Niederer, J.P.M., Versteeg, G.F., 2009. Structure and activity relationships for amine-based CO2 absorbents-II. Chemical Engineering Research and Design 87, 135-144.

Thitakamol, B., Veawab, A., 2008. Foaming Behavior in CO2 Absorption Process Using Aqueous Solutions of Single and Blended Alkanolamines. Industrial & Engineering Chemistry Research 47, 216-225.

Vincent E. Bower, R.A.R., and Roger G . Bates 1962. Acidic Dissociation Constant and Related Thermodynamic Quantities for Diethanolammonium Ion In Water From 0 to 50 °C. JOURNAL OF RESEARCH of the National Bureau of Standards A 66A, 71-75.

Xu, S., Wang, Y., Otto, F.D., Mather, A.E., 1992. Physicochemical properties of 2-piperidineethanol and its aqueous solutions. Journal of Chemical & Engineering Data 37, 407-411.

Yamada, H., Matsuzaki, Y., Chowdhury, F., Higashii, T., 2013. Computational investigation of carbon dioxide absorption in alkanolamine solutions. J. Mol. Model. 19, 4147-4153.

Yamada, H., Shimizu, S., Okabe, H., Matsuzaki, Y., Chowdhury, F.A., Fujioka, Y., 2010. Prediction of the Basicity of Aqueous Amine Solutions and the Species Distribution in the Amine−H2O−CO2 System Using the COSMO-RS Method. Industrial & Engineering Chemistry Research 49, 2449-2455.

Yang, Q., James, S., Ballard, M., Bown, M., 2012. Influence of Amine Chemical Structures to Amine Capacities in CO_2 Capture, Recent Advances in Post-Combustion CO_2 Capture Chemistry. American Chemical Society, pp. 29-42.